RESEARCH ARTICLE

# *BRAF* V600E, *TERT* promoter mutations and *CDKN2A/B* homozygous deletions are frequent in epithelioid glioblastomas: a histological and molecular analysis focusing on intratumoral heterogeneity

Nozomi Nakajima[1]; Sumihito Nobusawa ⓘ[1]; Satoshi Nakata[1,2]; Mitsutoshi Nakada[3]; Tatsuya Yamazaki[1]; Nozomi Matsumura[1]; Kenichi Harada[4]; Hadzki Matsuda[5]; Nobuaki Funata[6]; Shoichi Nagai[7]; Hideo Nakamura[8]; Atsushi Sasaki[9]; Jiro Akimoto[10]; Junko Hirato[11]; Hideaki Yokoo[1]

[1] Department of Human Pathology, Gunma University Graduate School of Medicine, Maebashi, Japan.
[2] Department of Neurosurgery, Gunma University Graduate School of Medicine, Maebashi, Japan.
[3] Department of Neurosurgery, Kanazawa University Graduate School of Medical Sciences, Kanazawa, Japan.
[4] Department of Human Pathology, Kanazawa University Graduate School of Medical Sciences, Kanazawa, Japan.
[5] Department of Neurosurgery, Dokkyo Medical University, Mibu, Japan.
[6] Department of Pathology, Tokyo Metropolitan Cancer and Infectious Diseases Center Komagome Hospital, Tokyo, Japan.
[7] Department of Neurosurgery Faculty of Medicine, University of Toyama, Toyama, Japan.
[8] Department of Neurosurgery, Kumamoto University Graduate School of Medical Sciences, Kumamoto, Japan.
[9] Department of Pathology, Saitama Medical University, Moroyama, Japan.
[10] Department of Neurosurgery, Tokyo Medical University, Tokyo, Japan.
[11] Department of Pathology, Gunma University Hospital, Maebashi, Japan.

## Abstract

Epithelioid glioblastoma (E-GBM) is a rare aggressive variant of IDH-wildtype glioblastoma newly recognized in the 2016 World Health Organization classification, composed predominantly of monotonous, patternless sheets of round cells with laterally positioned nuclei and plump eosinophilic cytoplasm. Approximately 50% of E-GBM harbor *BRAF* V600E, which is much less frequently found in other types of glioblastomas. Most E-GBM are recognized as primary/*de novo* lesions; however, several E-GBM with co- or pre-existing lower-grade lesions have been reported. To better understand associations between E-GBM and the lower-grade lesions, we undertook a histological and molecular analysis of 14 E-GBM, 10 of which exhibited lower-grade glioma-like components (8 E-GBM with co-existing diffuse glioma-like components, 1 E-GBM with a co-existing PXA-like component and 1 E-GBM with a pre-existing PXA). Molecular results demonstrated that the prevalence of *BRAF* V600E, *TERT* promoter mutations and *CDKN2A/B* homozygous deletions in E-GBM were 13/14 (93%), 10/14 (71%) and 11/14 (79%), respectively, and concurrent *BRAF* V600E, *TERT* promoter mutations and *CDKN2A/B* homozygous deletions were observed in 7/14 (50%) of E-GBM. These alterations were also frequently seen in the lower-grade lesions irrespective of the histology. Genetic analysis including array comparative genomic hybridization performed for 5 E-GBM with co- and pre-existing lower-grade components revealed that all molecular changes found in the lower-grade components were also observed in the E-GBM components, and additional changes were detected in the E-GBM components. In conclusion, E-GBM frequently exhibit *BRAF* V600E, *TERT* promoter mutations and *CDKN2A/B* homozygous deletions and these alterations tend to coexist in E-GBM. Taken together with the facts that only one PXA preceded E-GBM among these lower-grade lesions, and that co-occurrence of *BRAF* V600E, *TERT* promoter mutations and *CDKN2A/B* homozygous deletions have been reported to be rare in conventional lower-grade diffuse gliomas, the diffuse glioma-like components may be distinct infiltrative components of E-GBM, reflecting intratumoral heterogeneity.

# INTRODUCTION

Epithelioid glioblastoma (E-GBM) is a provisional uncommon variant of IDH-wildtype glioblastoma newly recognized in the 2016 World Health Organization (WHO) classification, characterized by a relatively solid aggregate of monotonous round epithelioid cells with abundant eosinophilic cytoplasm devoid of stellate processes, some eccentrically positioned nuclei, conspicuous nucleoli and distinct cellular membranes (9). E-GBM tend to occur in young adults and children, and the prognosis is particularly poor, even for glioblastomas, with an approximate median overall survival of 6 months (4, 9, 18, 19). From a genetic standpoint, approximately half of E-GBM harbor *BRAF* V600E, which is much less frequently found in other types of glioblastomas (9).

Although E-GBM are generally recognized as primary/*de novo* lesions (9), several E-GBM with a pre- or co-existent lower-grade components have been reported (1, 11, 18, 21, 22, 24, 28, 34, 35). The fact that most of these lower-grade lesions documented so far were pleomorphic xanthoastrocytomas (PXA) (1, 24, 34, 35) and that both tumors commonly exhibit *BRAF* V600E supports the possibility that E-GBM and PXA are related; the association was reinforced by a recent study identifying heterozygous deletion of *ODZ3* (*TEMN3*) as a shared genetic alteration, found in 7 of 11 E-GBM and 2 of 5 epithelioid PXA, defined therein as tumors composed predominantly of epithelioid cells with the same features as seen in E-GBM, but also demonstrating at least a small component of classic PXA (1). In addition, a few E-GBM with *BRAF* V600E have been reported to accompany a low-grade diffuse glioma-like component (11, 21, 22, 28).

In addition to *BRAF* V600E as a frequent genetic alteration in PXA, homozygous 9p21.3 deletions involving *CDKN2A/B* have been identified in 60%–83% of the cases (35, 38). Conversely, only a small number of E-GBM has been shown to harbor the homozygous deletions (1, 4, 28, 35), and the frequency in E-GBM is not clear.

Recently, we reported a case of E-GBM with a diffuse astrocytoma-like area demonstrating not only *BRAF* V600E but also *TERT* promoter mutations in both histologically distinct components (22); the prevalence of *TERT* promoter mutation in E-GBM is also not known, and that in PXA and diffuse astrocytoma has been reported to be 4 and 15%–32%, respectively (7, 8, 20).

In this report, we investigated 14 E-GBM, 10 of which exhibited pre- or co-existing lower-grade (WHO grade II/III) glioma-like lesions, and genetic associations between their E-GBM and lower-grade components were explored by molecular and cytogenetic analyses performed separately for each component, focusing on the status of *BRAF* V600E, *TERT* promoter mutations, *CDKN2A/B* deletions and *ODZ3* deletions.

# MATERIALS AND METHODS

## Tumor samples

Fourteen cases of E-GBM were collected for this study (Table 1). Six cases were previously reported (cases 2, 3, 5, 7, 8, 11) (11, 21, 22, 25, 28, 34). Five cases were from the consultation files of one of the authors (S.N.). Two cases were from the pathology archives of Department of Pathology, Gunma University Hospital. One case was from the pathology archives of Japan Brain Tumor Reference Center. Sections for histological and genetic analyses were prepared from formalin-fixed paraffin-embedded (FFPE) tissue specimens. This study was conducted in accordance with the Gunma University Ethical Committee.

## Conventional histological analysis

Three-micrometer-thick tissue sections were cut and stained with hematoxylin and eosin. Immunohistochemical staining was performed on FFPE tissue sections. Primary antibodies directed against the following antigens were applied: vimentin (V9; 1:200; Dako, Glostrup, Denmark), glial fibrillary acidic protein (GFAP; 1:5000) (27), Olig2 (1:5000) (40), cytokeratin (CAM5.2; 1:5; BD Bioscience, San Jose, CA, USA), p53 protein (monoclonal, 1:50; Leica Microsystems, Wetzlar, Germany), ATRX (polyclonal, 1:500; Sigma, St. Louis, MO, USA), BAF47/INI1 (BAF47; 1:100; BD Bioscience, San Jose, CA, USA), BRG1 (polyclonal; 1:1000; Millipore, Temecula, CA, USA) and Ki-67 (MIB-1; 1:100; Dako). For coloration, a commercially available biotin-streptavidin immunoperoxidase kit (Histofine, Nichirei, Tokyo, Japan) and diaminobenzidine were employed.

For vimentin, GFAP, Olig2, p53 and CAM5.2 the intensity of the staining was graded as negative, weak, moderate or strong and the extent was scored as follows: −, totally negative; 1+, <10% of tumor cells are positive; 2+, 10%–50% of tumor cells are positive; 3+, >50% of tumor cells are positive.

## DNA extraction

DNA was extracted from FFPE tissue sections, as previously described (29). For E-GBM cases with a lower-grade area (cases 1, 3–10), the extraction was performed separately from an E-GBM area and a lower-grade area.

## Array comparative genomic hybridization

Array comparative genomic hybridization (CGH) analysis was carried out using a 4 × 180 K CGH oligonucleotide microarray (Agilent Technologies, Santa Clara, CA, USA), as described previously (29). The sizes of gains and losses were refined by manual inspection of probe intensity plots. The log2 ratio of <−1.0 at the region of interest was considered to represent a homozygous deletion, and a value of −1.0 to −0.2 was considered to represent a heterozygous deletion (33).

## Direct DNA sequencing for *BRAF, IDH1/2, H3F3A, TP53* and *TERT* promoter mutations

Genomic DNA extracted from FFPE sections was amplified and sequenced using the primers described previously (2, 12, 26, 31, 36, 37). PCR products were sequenced on a 3130xl Genetic Analyzer (Applied Biosystems, Foster City, CA, USA) with the Big Dye Terminator v.1.1 Cycle Sequencing Kit (Applied Biosystems) following standard procedures.

## Multiplex ligation-dependent probe amplification analysis

Copy number changes in the *CDKN2A/B* genes, chromosomes 1 and 19 were analyzed by multiplex ligation-dependent probe amplification (MLPA) analysis. The SALSA MLPA probemix P088-C2

**Table 1.** Case list with clinical features.

| Case | Age (Yr)/Sex | Location | Histology | Radiation, dose | Chemotherapy | Local recurrence | Dissemination | Extra CNS metastasis | Clinical outcomes |
|---|---|---|---|---|---|---|---|---|---|
| 1 | 21/M | Temporo-parietal lobe | E-GBM with DA | Extended focal, 64.8 Gy | MCNU | NA | Yes | Scalp | Dead, 7months |
| 2[8] | 12/F | Temporal lobe | PXA | No | No | Yes | No | No | – |
| (Rec) | 25/F | Temporal lobe | E-GBM | Extended focal, 60 Gy | TMZ | NA | Yes | No | Dead, 4.3 months |
| 3[11] | 26/F | Frontal lobe | E-GBM with DA | Extended focal, 60 Gy | TMZ | No | Yes | Scalp | Dead, 2 months |
| 4 | 47/M | Parietal lobe | E-GBM with AA | NA | NA | NA | NA | NA | NA |
| 5[9] | 22/M | Occipital lobe | E-GBM with DA | Extended focal | TMZ+IFN | Yes | Yes | Vertebral bodies, lung thoracic wall, liver | Alive at 24 months |
| 6 | 32/M | Parietal lobe | E-GBM with PXA | Extended focal, 67 Gy | TMZ | No | No | No | Alive at 10 months |
| 7[10] | 18/M | Temporal lobe | E-GBM with DA | Whole brain, 40 Gy | TMZ+IFN | Yes | Yes | No | Dead, 2 months |
| 8[12] | 30/M | Temporal lobe, basal ganglia | E-GBM with OA | Yes | Yes | NA | NA | NA | Alive at 9 months |
| 9 | 70/M | Parietal lobe | E-GBM with DA | Extended focal, 40 Gy | TMZ | Yes | Yes | No | Dead, 7 months |
| 10 | 23/M | Frontal lobe | E-GBM with DA | Extended focal | PCZ+ACNU +VCR | Yes | Yes | Scalp | Dead, 3 months |
| 11[17] | 18/M | Temporal lobe | E-GBM | Extended focal | ACNU+IFN | Yes | Yes | No | Dead, 0.7 months |
| 12 | 32/F | Occipital lobe | E-GBM | Extended focal, 60 Gy | TMZ | No | No | No | Alive at 26 months |
| 13 | 47/M | Parietal lobe | E-GBM | 1st: Extended focal, 60 Gy 2nd: SRT | 1st: TMZ+IFN, 2nd: IFM +CDDP+VP16 | Yes | Yes | No | Dead, 25 months |
| 14 | 65/F | Frontal lobe | E-GBM | Extended focal, 60 Gy | TMZ | NA | NA | NA | Dead |

Abbreviations: Yr = years; M = male; F = female; Rec = recurrence; E-GBM = epithelioid glioblastoma; DA = diffuse astrocytoma; PXA = pleomorphic xanthoastrocytoma; AA = anaplastic astrocytoma; OA = oligoastrocytoma; NA = not avilable; MCNU = ranimustine; TMZ = temozolomide; IFN = interferon-beta; PCZ = procarbazine; ACNU = nimustine; VCR = vincristine; SRT = stereotactic radiotherapy; IFM = ifosfamide; CDDP = cisplatin; VP16 = etoposide.

(MRC-Holland, Amsterdam, the Netherlands) was used, and electrophoresis data were analyzed using Gene Mapper software (Life Technologies, Carlsbad, CA, USA) and normalized by Coffalyzer.net software (MRC-Holland). A dosage quotient (probe ratio) of between 0.4 and 0.7 was taken to be indicative of a heterozygous deletion, while a value < 0.4 was taken to represent a homozygous deletion (16).

### Fluorescence *in situ* hybridization analysis

Dual-probe hybridization using an intermittent microwave irradiation method was applied to 4-μm-thick FFPE tissue sections, as described previously (39). To investigate the copy number of *ODZ3*, a 4q34.3–4q35.1 probe was prepared from a bacterial artificial chromosome (BAC) clone, RP11–713O21, labeled with ENZO Orange-dUTP (Abbott Molecular Inc., Des Plaines, IL,

USA) and a 4p15.1 probe was prepared from a BAC clone RP11–81N11 labeled with ENZO Green-dUTP (Abbott Molecular Inc.). Metaphase fluorescence *in situ* hybridization (FISH) to verify clone mapping positions was performed using the peripheral blood cell cultures of a healthy donor.

## RESULTS

### Clinical data

Relevant clinical data are summarized in Table 1. Fourteen patients were between 18 and 70 years of age, with half of them being less than 30-year old. The female to male ratio was 10:4. All lesions were supratentorial. Thirteen patients presented with a primary lesion, and one patient had a previous history of PXA 13 years prior to the onset (case 2) (34). All 14 patients underwent surgical

**Table 2.** Histological, immunohistochemical, molecular and cytogenetic features.

| Case | Histology | Vascular wall invasion | Calcification | Epithelioid :spindle :lower grade† | Coagulative necrosis/ Palisading necrosis | Mitosis/ HPF | vimentin | GFAP | Olig2 | p53 | CAM5.2 | ATRX | INI1/ BRG1 | MIB-1 LI (%) | IDH1/2 | TP53 | BRAF | TERTp | CDKN2A (MLPA) | ODZ3 (FISH) |
|---|---|---|---|---|---|---|---|---|---|---|---|---|---|---|---|---|---|---|---|---|
| 1 | E-GBM | Present | – | 6:0:4 | Present/Absent | 3 | 3+ (s) | 1+ (m) | 2+ (m) | 2+ (w) | – | + | +/+ | 17.3 | – | – | + | C228T | Homo del* | LOH(–)* |
|  | DA | Absent | Present | | – | 0 | 2+ (w) | 3+ (m) | 3+ (m) | 2+ (w) | – | + | +/+ | 2.3 | – | – | + | C228T | Homo del* | LOH(–)* |
| 2³⁴ | E-GBM | Absent | Present | 10:0:0 | Present/Absent | 14 | 3+ (m) | 1+ (s) | 2+ (m) | 1+ (s) | – | + | +/+ | 48.4 | – | – | + | – | Homo del* | LOH(+)* |
|  | PXA | Absent | Present | 0:0:10 | – | 0 | 3+ (m) | 2+ (s) | 2+ (m) | 1+ (w) | – | + | +/+ | <1 | ND | – | + | ND | Homo del* | LOH(–)* |
| 3²¹ | E-GBM | Present | – | 6:0:4 | Present/Absent | 22 | 3+ (s) | 1+ (s) | 1+ (m) | 1+ (w) | – | + | +/+ | 62.6 | – | – | + | C228T | Homo del* | LOH(–)* |
|  | DA | Absent | Present | | – | 0 | 1+ (m) | 3+ (m) | 3+ (s) | – | – | + | +/+ | <1 | – | – | + | – | No CNA* | LOH(–)* |
| 4 | E-GBM | Present | – | 7:0:3 | Present/Absent | 15 | 3+ (s) | 3+ (s) | 2+ (m) | 1+ (m) | – | – | +/+ | 24.1 | ND | ND | + | – | Homo del* | LOH(–)* |
|  | AA | Absent | Present | | – | 4 | 3+ (s) | 3+ (s) | 3+ (s) | 1+ (m) | – | – | +/+ | 5.1 | – | ND | + | – | Homo del* | LOH(–)* |
| 5²⁸ | E-GBM | Present | – | 18:1:1 | Present/Absent | 15 | 3+ (s) | 1+ (m) | 1+ (w) | 1+ (w) | – | + | +/+ | 23.8 | – | – | + | C228T | Homo del* | LOH(+)* |
|  | DA | Absent | – | | – | 0 | 1+ (w) | 3+ (m) | 2+ (w) | 1+ (w) | – | + | +/+ | 2.9 | – | – | + | C228T | Homo del* | LOH(–)* |
| 6 | E-GBM | Present | Absent | 9:0:1 | Present/Absent | 4 | 3+ (m) | 2+ (s) | 2+ (s) | 2+ (m) | 1+ (w) | + | +/+ | 16.3 | – | – | + | C228T | Homo del | LOH(–) |
|  | PXA | Absent | Absent | | – | 0 | 3+ (s) | 3+ (s) | 3+ (m) | 1+ (m) | – | + | +/+ | 2.3 | – | – | + | C228T | Homo del | LOH(–) |
| 7²² | E-GBM | Present | – | 7:1:2 | Present/Absent | 32 | 3+ (s) | 1+ (s) | 2+ (m) | 2+ (m) | 2+ (s) | + | +/+ | 45.8 | – | – | + | C228T | Homo del | LOH(–) |
|  | DA | Absent | Absent | | – | 1 | 2+ (m) | 3+ (m) | 3+ (s) | 1+ (w) | – | + | +/+ | 1.6 | – | – | + | C228T | Homo del | LOH(–) |
| 8¹¹ | E-GBM | Present | – | 6:3:1 | Present/Absent | 5 | 3+ (s) | 1+ (s) | 2+ (m) | 1+ (w) | 2+ (m) | + | +/+ | 17.7 | – | – | + | C228T | Homo del | LOH(–) |
|  | OA | Absent | Present | | – | 0 | 3+ (s) | 3+ (s) | 3+ (s) | 1+ (w) | – | + | +/+ | 3.7 | – | – | + | C228T | Homo del | LOH(–) |
| 9 | E-GBM | Present | – | 7:0:3 | Present/Absent | 9 | 3+ (s) | 1+ (s) | 1+ (w) | 1+ (m) | 1+ (w) | + | +/+ | 35.5 | – | – | + | C250T | Homo del | LOH(–) |
|  | DA | Absent | Present | | – | 0 | 1+ (m) | 3+ (s) | 3+ (s) | 1+ (w) | – | + | +/+ | 3.3 | – | – | + | C250T | No CNA | LOH(–) |
| 10 | E-GBM | Present | – | 6:3:1 | Present/Present | 15 | 3+ (s) | 1+ (s) | 1+ (m) | 2+ (s) | – | + | +/+ | 17.7 | – | c.633delT p.R213fs*34 | + | C228T | No CNA | LOH(–) |
|  | DA | Absent | Present | | – | 0 | 1+ (w) | 3+ (m) | 2+ (s) | 1+ (m) | – | + | +/+ | <1 | – | – | + | – | No CNA | LOH(–) |
| 11²⁵ | E-GBM | Present | – | 10:0:0 | Present/Present | 9 | 3+ (s) | 1+ (m) | 1+ (w) | 1+ (w) | – | ND | +/+ | 27.1 | – | – | + | C228T | No CNA | LOH(–) |
| 12 | E-GBM | Present | – | 7:3:0 | Present/Absent | 4 | 3+ (m) | 1+ (m) | 3+ (s) | 2+ (m) | 2+ (m) | + | +/+ | 18.0 | – | – | + | – | Homo del | LOH(–) |
| 13 | E-GBM | Present | – | 9:1:0 | Present/Present | 19 | 1+ (s) | 1+ (s) | – | 2+ (s) | 1+ (s) | + | +/+ | 30.4 | – | c.742C>A p.R248R | – | C228T | No CNA | LOH(–) |
| 14 | E-GBM | Present | – | 8:2:0 | Present/Absent | 18 | 3+ (m) | 1+ (s) | 3+ (m) | 1+ (m) | – | + | +/+ | 20.7 | – | – | + | – | Homo del | LOH(–) |

The intensity and extent of immunopositive tumor cells were scored as follows: w = weak; m = moderate; s = strong; –, totally negative; 1+, <10%; 2+, 10–50%; 3+, >50%.

*The results of FISH and MLPA analyses were compatible with array CGH data.

†The areas of epithelioid, anaplastic spindle and lower grade glioma components were estimated.

Abbreviations: HPF = high power field; GFAP = glial fibrillary acidic protein; Olig2 = oligodendrocyte transcription factor 2; MIB-1 LI = MIB-1 labeling index; FISH = fluorescence in situ hybridization; dPCR = digital polymerase chain reaction; IDH = Isocitrate dehydrogenase; TERTp = Telomerase reverse transcriptase promoter; E-GBM = epithelioid glioblastoma; DA = diffuse astrocytoma; PXA = pleomorphic xanthoastrocytoma; AA = anaplastic astrocytoma; OA = oligoastrocytoma; LOH = loss of heterozygosity; Homo del = homozygous deletion; CNA = copy number aberration; ND = not detected.
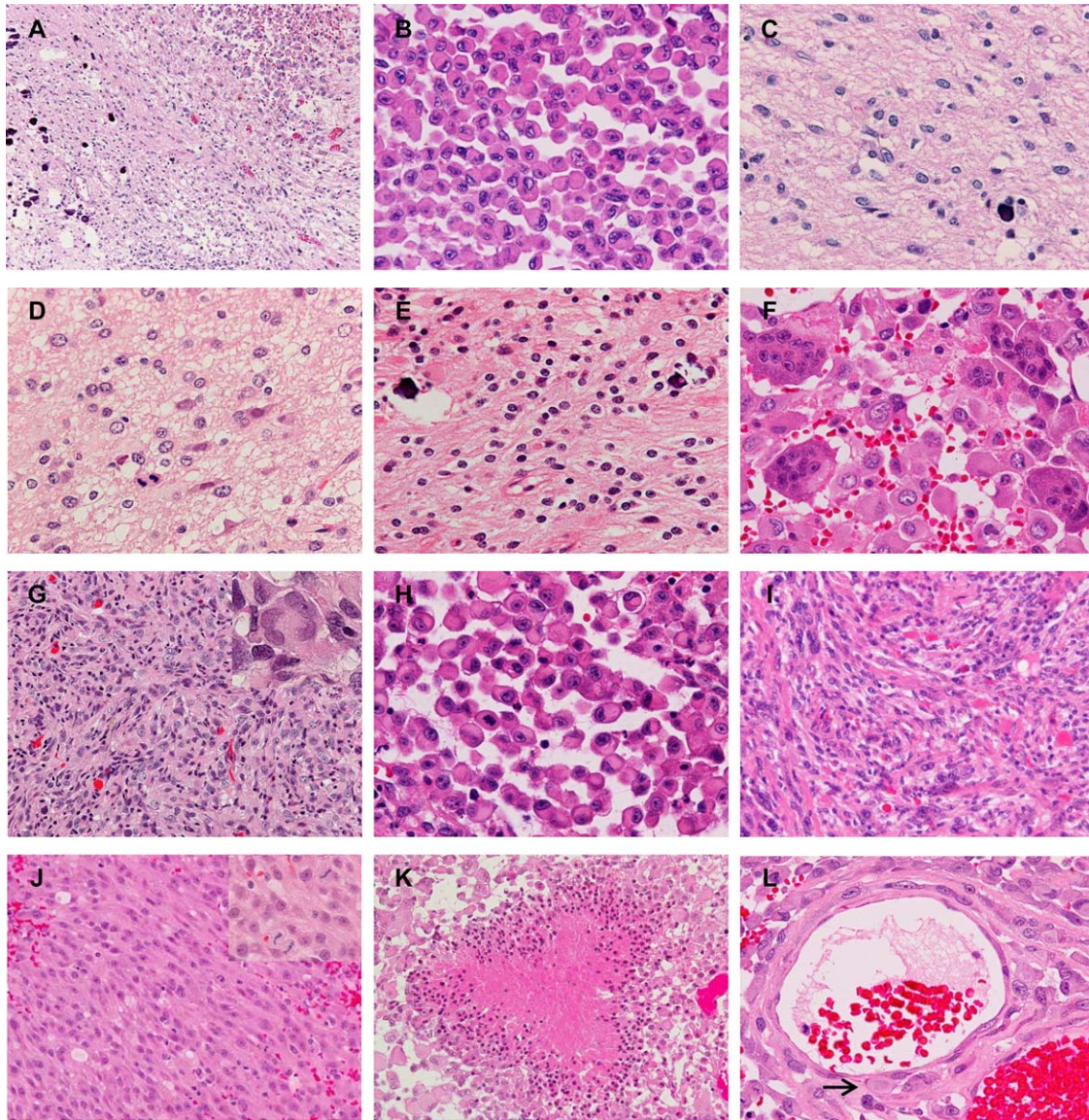
**Figure 1.** *Microscopic appearance.* **A–C.** Epithelioid glioblastoma (E-GBM) and diffuse astrocytoma (DA)-like components in case 9. The interface between the E-GBM (top right) and DA-like (bottom left) components is relatively sharp **(A)**. Note the calcification in the DA-like component **(A,C)**. The E-GBM area is composed of monotonous, discohesive round cells with laterally positioned nuclei and eosinophilic cytoplasm **(B)**. The DA-like component exhibits mild cellular proliferation of well-differentiated neoplastic fibrillary astrocytes **(C)**. **D.** The anaplastic astrocytoma-like component in case 4, presenting 4 mitoses per 10 high-power fields. **E,F.** The oligoastrocytoma-like component with calcification **(E)** and osteoclast-like giant cells intermingled with epithelioid tumor cells **(F)** in case 8. **G.** The PXA-like component in case 6 shows a fascicular arrangement of spindle-shaped cells with some multinucleated pleomorphic cells (inset). **H,I.** E-GBM **(H)** and its precursor PXA lesion **(I)** in case 2. The PXA shows numerous eosinophilic granular bodies **(I)**. **J.** A component with anaplastic spindle-shaped cells with monotonous nuclei and thick processes (case 12). Frequent mitosis is seen (inset). **K.** Palisading necrosis in the E-GBM component (case 10). **L.** Epithelioid tumor cells invade the vascular wall in the subarachnoid space (case 6). The arrow indicates a tumor cell right beneath the endothelium. Original magnification: **A**, x100; **G, I–K**, x200; **B–F, H, L inset in G and J**, x400.

resection, and 12 of these cases with available clinical data received subsequent chemoradiotherapy with temozolomide or other alkylating agents. Cerebrospinal fluid dissemination and extra-CNS metastasis were documented in ten and three cases, respectively. Of 14 cases, 10 had sufficient clinical follow-up to evaluate outcomes. Of these, seven patients (cases 1–3, 7, 9–11) died of disease within 7 months after the surgery due to the early tumor dissemination,

whereas three patients (cases 5, 12, 13) survived over 2 years with or without local recurrence.

## Histopathological findings

The histological features are summarized in Table 2 (Figure 1A–L). Nine of 14 E-GBM exibited co-existing lower-grade

components: E-GBM with a diffuse astrocytoma-like component (cases 1, 3, 5, 7, 9, 10; Figure 1A–C), E-GBM with an anaplastic astrocytoma-like component (case 4; Figure 1D), E-GBM with an oligoastrocytoma-like component (case 8; Figure 1E,F) or E-GBM with a PXA-like component (case 6; Figure 1G). The interface between E-GBM and lower-grade components was relatively sharp in cases 3, 5, 6, 8–10 (Figure 1A) and intraparenchymal and perivascular calcifications were frequently observed in these lower-grade areas (cases 1–4, 8–10; Figure 1A,C,E).

All E-GBM in this study were mainly composed of monotonous, discohesive sheets of epithelioid cells with eosinophilic, rounded cytoplasm lacking processes (Figure 1B,H). The nuclei were large, laterally positioned, and variable in shape; round, ovoid, reniform or crescent nuclei with distinct nucleoli were observed. The cytoplasm often contained filamentous-like or hyalinized inclusions with or without fine basophilic granules, and small cytoplasmic vacuoles were also found in some tumor cells. Unlike conventional GBMs, an interspersed fibrillary matrix was not observed between these tumor cells. Mitotic figures were frequent. In case 8, there were numerous osteoclast-like giant cells intermingling with epithelioid cells (Figure 1F) (11).

In diffuse astrocytoma-like components, a mildly cellular proliferation of glial tumor cells with oval to irregular nuclei and cytoplasmic processes, in the background of a loosely structured matrix were observed (cases 1, 3–5, 7, 9, 10; Figure 1C). Subpial and perineuronal accumulation of tumor cells, indicating the infiltrative nature of the tumor cells, were observed in some cases. Mitotic figures were scant (case 7) or absent (cases 1, 3, 5, 9, 10). A lower-grade component of case 4 showed similar histology but exhibited 4 mitotic figures per 10 high-power fields, meeting the criteria for "anaplastic" astrocytoma (Figure 1D). In a oligoastrocytoma-like component in case 8, fibrillary astrocytic tumor cells and oligodendroglial tumor cells with a perinuclear halo were intimately mixed (Figure 1E), where no mitotic figures were observed.

In case 6, a PXA-like component co-existing with E-GBM demonstrated a fascicular arrangement of spindle-shaped cells with some mononucleated or multinucleated pleomorphic cells (Figure 1G). Perivascular lymphocytic cuffings and intercellular reticlin meshwork were noted, although eosinophilic granular bodies (EGBs) could not be identified. Mitotic figures were not observed.

The pre-existing PXA lesion in case 2 was composed of a combination of spindle-shaped, xanthic and pleomorphic, multinucleated giant astrocytes, with numerous EGBs, perivascular lymphocytic cuffings and abundant reticulin meshwork (Figure 1I).

In addition to the typical E-GBM areas, seven cases contained another anaplastic area composed of spindle-shaped cells with relatively monotonous nuclei and thick processes (cases 5, 7, 8, 10, 12–14; Figure 1J). Characteristics of localized astrocytomas (PXA and pilocytic astrocytoma) as follows were not observed: piloid cytoplasmic processes, xanthomatous change, Rosenthal fibers or EGBs. These areas were not regarded as lower-grade components because of frequent mitosis, albeit less than in the E-GBM components and necrosis seen in these components.

In areas of these epithelioid and anaplastic spindle-shaped cells, coagulative necrosis was observed in all cases, whereas palisading necrosis was identified in three cases (cases 10, 11, 13; Figure 1K), and microvascular proliferation was absent in all cases. These tumor cells tended to extend within the subarachnoid space, and in most cases, characteristic vascular wall invasion (Figure 1L) and intratumoral hemorrhage were observed.

The immunohistochemical findings are summarized in Table 2 (Figure 2A–L). E-GBM exhibited diffuse and strong staining with vimentin (Figure 2A). GFAP immunoreactivity was identified in a limited number of epithelioid cells with a few cytoplasmic processes (Figure 2B), but was diffusely observed in lower-grade glioma cells (Figure 2C). Anaplastic spindle-shaped cells were generally sparsely immunostained for GFAP (Figure 2D). Nuclear Olig2 staining was variable in extent in epithelioid cells; mostly negative in cases 5, 9, 11 and 13 (Figure 2E), whereas diffusely positive in cases 12 and 14 (Figure 2F). Most E-GBM showed weak to moderate p53 immunoreactivity (Figure 2G), but in cases 10 and 13, strong immunostaining was observed (Figure 2H). CAM5.2 staining was focally observed in epithelioid cells in case 6–9, 12–14. The loss of ATRX nuclear expression was detected only in case 4 (Figure 2I). The retention of nuclear staining of INI1 and BRG1 was observed throughout the specimen in all cases (Figure 2J). MIB-1 staining depicted markedly higher proliferation indexes in the E-GBM components (Figure 2K) than those in the lower-grade components (Figure 2L).

## Genetic analysis

The results of genetic analysis are summarized in Table 2. The prevalence of BRAF V600E, TERT promoter mutations and CDKN2A/B homozygous deletions (Supporting Information Figure S1A) detected by direct DNA sequencing or MLPA analysis in our cohort of E-GBM were 13/14 (93%), 10/14 (71%) and 11/14 (79%), respectively. Concurrent BRAF V600E, TERT promoter mutations and CDKN2A/B homozygous deletions were observed in 7 of 14 E-GBM (50%; cases 1, 3, 5–9). These 7 E-GBM were with co-existing lower-grade lesions, of which five cases demonstrated the same combination of alterations in their lower-grade lesions, whereas none of these alterations were detected in the diffuse astrocytoma-like area of case 3, and a CDKN2A/B homozygous deletion could not be detected in the diffuse astrocytoma-like area of case 9.

FISH analysis detected loss of heterozygosity (LOH) of ODZ3 in the E-GBM components of 2/14 cases (cases 2, 5), but not in their lower-grade components (Supporting Information Figure S1B).

The results of array CGH revealed that all copy number alterations (CNA) observed in the lower-grade lesions were also detected in the E-GBM components in all five cases analyzed (Figure 3, Supporting Information Table S1). CNA recurrently found only in the E-GBM components but not in the lower-grade lesions were a gain on 3q24 - q26.2 (cases 1, 2), a heterozygous deletion on 4q34.3 - q35.1 involving ODZ3 (cases 2, 5; Figure 3C), a heterozygous deletion on 6q11.1 - q22.33 (cases 2, 3), a heterozygous deletion on 6q23.3 - q24.1 (cases 2, 3), a gain on whole chromosome 7 (cases 1, 3) and a gain on 7q33 - q36.3 (cases 1–3). A homozygous deletion on 3q13.31 involving LSAMP detected only in the E-GBM component of case 5, which we previously reported (28), was not observed in any other cases. Small homozygous deletions on 4q13.2 (cases 1, 5), 8p11.22 involving ADAM3A and ADAM5 (cases 3, 4), and 22q11.23 involving GSTT1 and GSTTP2 (cases 3, 5), and a small gain on 6p22.1 (cases 1, 4) recurrently found both in the E-GBM and
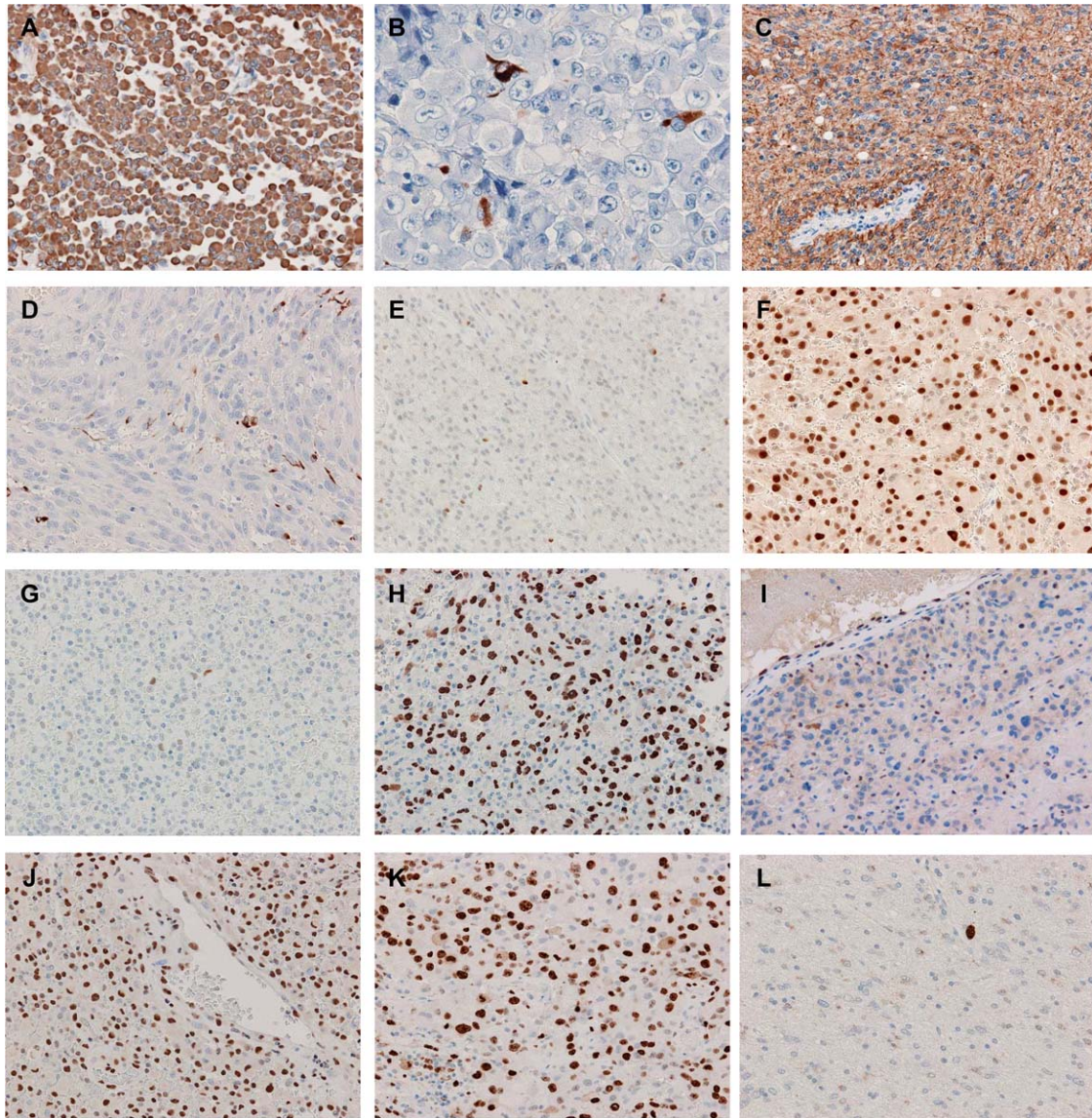
**Figure 2.** *Immunohistochemistry.* **A.** Vimentin is diffusely and strongly positive in E-GBM (case 9). **B,C.** A limited number of epithelioid cells with a few cytoplasmic processes are positive for GFAP **(B)**, and the DA-like area is diffusely positive **(C)** in case 7. **D.** Anaplastic spindle-shaped cells are sparsely immunostained with GFAP (case 5). **E,F.** The extent and intensity of nuclear Olig2 staining is variable in the E-GBM components; few and moderate in case 3 **(E)**, whereas diffuse and strong in case 12 **(F)**. **G,H.** The E-GBM area has sparse and weak p53 immunoreactivity in case 3 **(G)**, but diffuse and strong in case 13 **(H)**. **I.** The loss of ATRX nuclear expression in case 4 (E-GBM area). **J.** The nuclear staining of INI1 is retained (E-GBM area of case 3). **K,L.** The MIB-1 labeling index is approximately 60% in the E-GBM component **(K)** and less than 1% in the DA-like component **(L)** in case 3. Original magnification: **A**, **C–L**, x200; **B**, x400.

lower-grade components were in regions of known benign copy number variants (polymorphisms) reported in the Database of Genomic Variants (DGV; http://dgv.tcag.ca/dgv/app/home). The results of CNA involving *CDKN2A/B* and *ODZ3* were compatible with the results of MLPA and FISH analyses, respectively (Table 2, Figure 3, Supporting Information Figure S1). As for loss of other important tumor suppressor genes, a heterozygous deletion on 13q involving *RB1* was found only in the E-GBM component of case 2, a heterozygous deletion on 10q involving *PTEN* was found both in the E-GBM and diffuse astrocytoma-like components of case 1 and only in the E-GBM component of case 4, and

a heterozygous deletion on 17p involving *TP53* was found only in the E-GBM component of case 2 (Figure 3, Supporting Information Figure S1).

No *IDH1/2* or *H3F3A* mutation or 1p/19q loss was observed in any cases analyzed (Supporting Information Figure S1A). *TP53* mutations were found in two cases: a frameshift mutation (c.633delT, pR213fs*34) only in the E-GBM component of case 10, and a silent mutation in codon 248 hot spot (c.742C > A, p.R248R) in case 13, both of which are reported in the Catalogue of Somatic Mutations in Cancer (COSMIC) database (http://cancer.sanger.ac.uk/cosmic; Table 2).
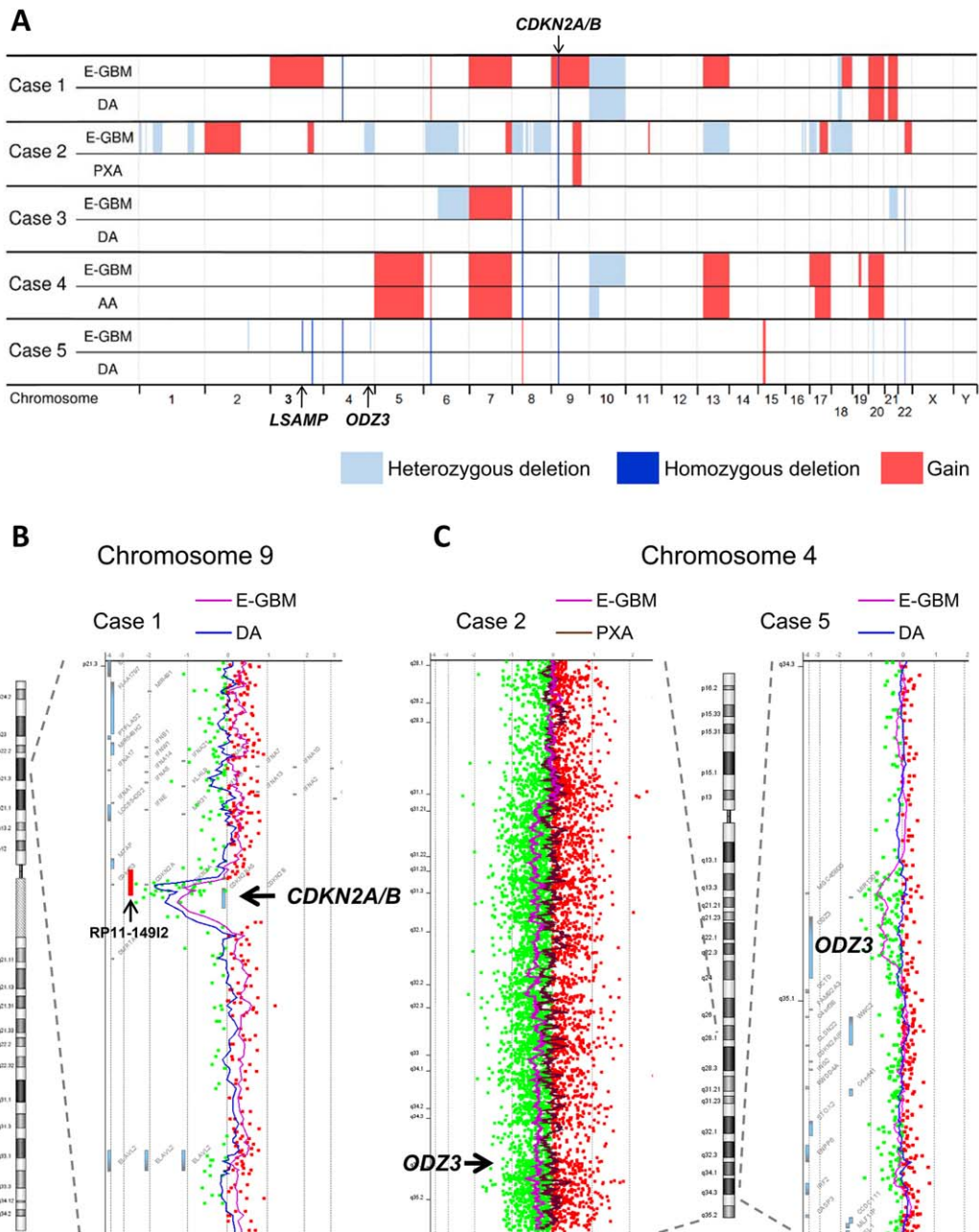
**Figure 3.** *Results of array comparative genomic hybridization (CGH).* **A.** Copy number alterations (CNA) detected by array CGH performed separately for the E-GBM components and lower-grade lesions in cases 1–5 are visualized. All CNA observed in the lower-grade lesions were also detected in the E-GBM components in all cases. Homozygous deletions involving *CDKN2A/B* were found both in the E-GBM components and lower-grade lesions in cases 1, 2, 4 and 5, but only in the E-GBM component in case 3. Several CNA were recurrently found only in the E-GBM components, including a heterozygous deletion on 4q34.3 - q35.1 involving *ODZ3* (cases 2, 5). **B.** A homozygous deletion involving *CDKN2A/B* in case 1. Chromosome 9 except the deleted region demonstrated a low-level gain in the E-GBM component. The positions of *CDKN2A/B* and a bacterial artificial chromosome clone RP11–149I2, which is commonly used for fluorescence *in situ* hybridization analysis for investigating the copy number of *CDKN2A/B*, are indicated. **C.** Heterozygous deletion involving *ODZ3* observed only in the E-GBM components of cases 2 and 5. The position of *ODZ3* is indicated.

Abbreviations: E-GBM = epithelioid glioblastoma; DA = diffuse astrocytoma-like component; PXA = pleomorphic xanthoastrocytoma.

## DISCUSSION

Histologically and molecularly, PXA, particularly anaplastic PXA, has been known to be related with E-GBM (9, 13). PXA and

E-GBM often share such features as a relatively solid growth pattern, dural attachment and reticulin-rich areas, and it has been noted that a subset of anaplastic PXA show similar histologic features to

E-GBM, but E-GBM usually possess more cytologically uniform cells and lack eosinophilic granular bodies unlike anaplastic PXA (1, 17–19). From a genetic stand point, our results suggest that, although *BRAF* mutations and *CDKN2A/B* homozygous deletions are common in E-GBM and PXA, the frequency of *TERT* promoter mutation is a definite difference between these tumors compared with the reported frequency in PXA. Investigating 14 E-GBM, the prevalence of *BRAF* V600E, *TERT* promoter mutations and *CDKN2A/B* homozygous deletions in our cohort were 13/14 (93%), 10/14 (71%) and 11/14 (79%), respectively, and concurrent *BRAF* V600E, *TERT* promoter mutations and *CDKN2A/B* homozygous deletions were observed in 7/14 (50%) of E-GBM (Table 2). *BRAF* mutations and *CDKN2A/B* homozygous deletions are common in PXA (50%–78% and 60%–83%, respectively) (14, 35, 38), whereas, according to a single study, *TERT* promoter mutations were found in 1/25 (4%) and 3/13 (23%) of PXA and anaplastic PXA, respectively (20). It is of note that, although frequent *BRAF* V600E, *TERT* promoter mutations and *CDKN2A/B* deletions have not been reported so far in any other CNS tumor, this combination of alterations was observed in a subset of melanomas (approximately 11%) (15), and morphological similarities between E-GBM and melanomas have been pointed out (4, 18, 19).

Although most of the previously reported pre- or co-existent lower-grade lesions with E-GBM have been PXA, 8 out of 10 in our present cohort were diffuse gliomas: diffuse astrocytoma-like components in six cases, an anaplastic astrocytoma-like component in one case and an oligoastrocytoma-like component in one case. *BRAF* V600E, *TERT* promoter mutations and *CDKN2A/B* homozygous deletions were also frequently observed in these lower-grade lesions; however, *IDH1/2* mutations, genetic characteristics of lower-grade diffuse gliomas, were not observed in any lesion (Table 2). H3 K27M mutation has been reported in two cases of E-GBM in the thalamus and spine, the former also harboring *BRAF* V600E, but *H3F3A* K27M mutation was not detected in our present cohort (1, 4).

In the current study, we compared the epithelioid cell and infiltrative lower-grade areas of E-GBM in regards to their histology, and they were distinguished in terms of cytological features, growth patterns (infiltrative or relatively solid), proliferative ability and immunohistochemical findings (GFAP in particular). Calcification was seen not only in a oligoastrocytoma-like area (case 8) but also even in five diffusely infiltrating astrocytoma-like areas of 7 E-GBM cases (cases 1, 3, 4, 9, 10); calcification, a feature associated with slow growth, is a common histological finding in oligodendroglial tumors, but is uncommon in diffuse astrocytomas (5).

Co-occurrence of *BRAF* V600E, *TERT* promoter mutations and *CDKN2A/B* homozygous deletions are rare in diffuse gliomas. Among 491 grades II–III diffuse gliomas in recent reports mostly composed of adult cases (3, 6, 41), no cases shared *BRAF* V600E, *TERT* promoter mutations and *CDKN2A/B* homozygous deletions. As for glioblastomas (302 cases), seven cases had both *BRAF* and *TERT* promoter mutations, of which three cases also had *CDKN2A/B* homozygous deletions; however, epithelioid cell morphology was not mentioned in these series. Meanwhile, concurrent *BRAF* mutation and *CDKN2A* homozygous deletion have been found in a subset of diffuse astrocytomas in children and young adults (10, 30). Mistry *et al* reported that *BRAF* mutations and *CDKN2A* deletions (heterozygous or homozygous) constitute a clinically distinct subtype of secondary high-grade gliomas (sHGG) transforming

from pediatric low-grade gliomas (PLGG) (23). These transforming PLGG included "low-grade astrocytomas," pilocytic astrocytomas, PXA and gangliogliomas, and 2 of them (a low grade astrocytoma and a ganglioglioma) had *TERT* promoter mutations in addition to *BRAF* mutations and *CDKN2A* deletions; however, epithelioid cell morphology was not mentioned in relation to sHGG (23). Together with the fact that no E-GBM was preceded by a lower-grade diffuse glioma in the current series, the lower-grade diffuse glioma-like areas may be distinct infiltrative components of E-GBM, reflecting intratumoral heterogeneity.

The exception is case 3, where *BRAF* V600E, *TERT* promoter mutations and *CDKN2A/B* homozygous deletions were found in the E-GBM component, but none of these alterations were detected in the diffuse astrocytoma-like component. Moreover, although 2 CNA found in the diffuse astrocytoma-like component were also detected in the E-GBM component using array CGH (Figure 3A, Supporting Information Table S1), these CNA may be benign copy number variants (polymorphisms); therefore, we could not detect any possible somatic genetic changes in the diffuse astrocytoma-like component, and could not reveal a genetic association between these 2 components. Unrelated E-GBM and diffuse astrocytoma may present as a collision tumor in this case; however, if not, underlying more pathogenetically important alterations may be shared both in these components, which could not be detected by the methods used in this study.

In the current study, areas of anaplastic spindle-shaped cells with relatively monotonous nuclei, a solid growth pattern, decreased GFAP staining and devoid of characteristics of localized astrocytomas (PXA and pilocytic astrocytoma) were found in 7 E-GBM (Figure 2D, Table 2). This finding has not been featured in relation to E-GBM, but can be a frequent element in E-GBM. Another histological characteristic of E-GBM is tumor cell invasion into the wall of vessels in the subarachnoid space, which was observed in 13 cases in the present study. This characteristic, together with the discohesiveness of tumor cells, may be associated with the extra-CNS metastasis, leptomeningeal dissemination and extensive intratumoral hemorrhage (21, 28).

Case 4 is the first E-GBM with loss of nuclear ATRX expression ever reported (Figure 2I, Table 2). ATRX expression is almost invariably lost in the setting of *ATRX* mutations, and the mutations are frequently observed in IDH-mutant diffuse astrocytomas and anaplastic astrocytomas (8). A small portion of E-GBM may exhibit *ATRX* mutations mutually exclusively with *TERT* promoter mutations as in diffuse gliomas (8).

For investigating the copy number of *CDKN2A/B* by FISH analysis, the BAC clone RP11–149I2 is commonly used; however, the position of the BAC clone does not fit into the homozygously deleted regions in 3 of 5 E-GBM (cases 1, 4, 5) detected by array CGH (Figure 3B, Supporting Information Table S1). We tested FISH analysis using the BAC clone for the five cases analyzed by array CGH, and validated the deletions in cases 2 and 3, but could not in the cases 1, 4, 5 (data not shown). Deleted regions involving *CDKN2A/B* in E-GBM may be narrower, as seen in other tumors (32); therefore, other methods such as MLPA and array-based analysis may be suitable, the former being more appropriate for routine use and screening large cohorts.

In conclusion, our results show that E-GBM frequently exhibit *BRAF* V600E, *TERT* promoter mutations and *CDKN2A/B* homozygous deletions, these alterations tend to coexist in E-GBM, and that

diffuse glioma-like components as well as PXA-like components are commonly observed in E-GBM. Although PXA can rarely secondarily progress to E-GBM, the diffuse glioma-like components may reflect intratumoral heterogeneity. Further studies with large cohorts are needed to better understand the pathogenesis of E-GBM.

# REFERENCES

1. Alexandrescu S, Korshunov A, Lai SH, Dabiri S, Patil S, Li R *et al* (2016) Epithelioid glioblastomas and anaplastic epithelioid pleomorphic xanthoastrocytomas–same entity or first cousins? *Brain Pathol* **26**:215–223.

2. Arai M, Nobusawa S, Ikota H, Takemura S, Nakazato Y (2012) Frequent IDH1/2 mutations in intracranial chondrosarcoma: a possible diagnostic clue for its differentiation from chordoma. *Brain Tumor Pathol* **29**:201–206.

3. Arita H, Yamasaki K, Matsushita Y, Nakamura T, Shimokawa A, Takami H *et al* (2016) A combination of TERT promoter mutation and MGMT methylation status predicts clinically relevant subgroups of newly diagnosed glioblastomas. *Acta Neuropathol Commun* **4**:79.

4. Broniscer A, Tatevossian RG, Sabin ND, Klimo P, Jr, Dalton J, Lee R *et al* (2014) Clinical, radiological, histological and molecular characteristics of paediatric epithelioid glioblastoma. *Neuropathol Appl Neurobiol* **40**:327–336.

5. Burger PC, Scheithauer BW (2007) Diffuse astrocytoma. In: *AFIP Atlas of Tumor Pathology Fourth Series Fascicle 7, Tumors of the Central Nervous System*. SG Silverberg, LH Sobin (eds), p. 48. Armed Forces Institute of pathology: Washington, DC.

6. Ceccarelli M, Barthel FP, Malta TM, Sabedot TS, Salama SR, Murray BA *et al* (2016) Molecular profiling reveals biologically discrete subsets and pathways of progression in diffuse glioma. *Cell* **164**: 550–563.

7. Chan AK, Yao Y, Zhang Z, Chung NY, Liu JS, Li KK *et al* (2015) TERT promoter mutations contribute to subset prognostication of lower-grade gliomas. *Mod Pathol* **28**:177–186.

8. Eckel-Passow JE, Lachance DH, Molinaro AM, Walsh KM, Decker PA, Sicotte H *et al* (2015) Glioma groups based on 1p/19q, IDH, and TERT promoter mutations in tumors. *N Engl J Med* **372**: 2499–2508.

9. Ellison DW, Kleinschmidt-DeMasters BK, Park SH (2016) Epithelioid glioblastoma. In: *WHO Classification of Tumors of the Central Nervous System*, 4th edn. DN Louis, H Ohgaki, OD Wiestler, WK Cavenee (eds), pp. 50–51. IARC Press: Lyon.

10. Forshew T, Tatevossian RG, Lawson AR, Ma J, Neale G, Ogunkolade BW *et al* (2009) Activation of the ERK/MAPK pathway: a signature genetic defect in posterior fossa pilocytic astrocytomas. *J Pathol* **218**: 172–181.

11. Funata N, Nobusawa S, Yamada R, Shinoura N (2016) A case of osteoclast-like giant cell-rich epithelioid glioblastoma with BRAF V600E mutation. *Brain Tumor Pathol* **33**:57–62.

12. Gessi M, van de Nes J, Griewank K, Barresi V, Buckland ME, Kirfel J *et al* (2014) Absence of TERT promoter mutations in primary melanocytic tumours of the central nervous system. *Neuropathol Appl Neurobiol* **40**:794–797.

13. Giannini C, Paulus W, Louis DN, Liberski PP, Figarella-Branger D, Capper D (2016) Anaplastic pleomorphic xanthoastrocytoma. In: *WHO Classification of Tumors of the Central Nervous System*, 4th edn. DN Louis, H Ohgaki, OD Wiestler, WK Cavenee (eds), pp. 98–99. IARC Press: Lyon.

14. Giannini C, Paulus W, Louis DN, Liberski PP, Figarella-Branger D, Capper D (2016) Pleomorphic xanthoastrocytoma. In: *WHO Classification of Tumors of the Central Nervous System*, 4th edn. DN Louis, H Ohgaki, OD Wiestler, WK Cavenee (eds), pp. 94–97. IARC Press: Lyon.

15. Hayward NK, Wilmott JS, Waddell N, Johansson PA, Field MA, Nones K *et al* (2017) Whole-genome landscapes of major melanoma subtypes. *Nature* **545**:175–180.

16. Jeuken J, Sijben A, Alenda C, Rijntjes J, Dekkers M, Boots-Sprenger S *et al* (2009) Robust detection of EGFR copy number changes and EGFR variant III: technical aspects and relevance for glioma diagnostics. *Brain Pathol* **19**:661–671.

17. Kepes JJ (1993) Pleomorphic xanthoastrocytoma: the birth of a diagnosis and a concept. *Brain Pathol* **3**:269–274.

18. Kleinschmidt-DeMasters BK, Aisner DL, Birks DK, Foreman NK (2013) Epithelioid GBMs show a high percentage of BRAF V600E mutation. *Am J Surg Pathol* **37**:685–698.

19. Kleinschmidt-DeMasters BK, Alassiri AH, Birks DK, Newell KL, Moore W, Lillehei KO (2010) Epithelioid versus rhabdoid glioblastomas are distinguished by monosomy 22 and immunohistochemical expression of INI-1 but not claudin 6. *Am J Surg Pathol* **34**:341–354.

20. Koelsche C, Sahm F, Capper D, Reuss D, Sturm D, Jones DT *et al* (2013) Distribution of TERT promoter mutations in pediatric and adult tumors of the nervous system. *Acta Neuropathol* **126**:907–915.

21. Kuroda J, Nobusawa S, Nakamura H, Yokoo H, Ueda R, Makino K *et al* (2016) A case of an epithelioid glioblastoma with the BRAF V600E mutation colocalized with BRAF intact low-grade diffuse astrocytoma. *Neuropathology* **36**:181–186.

22. Matsumura N, Nakajima N, Yamazaki T, Nagano T, Kagoshima K, Nobusawa S *et al* (2017) Concurrent TERT promoter and BRAF V600E mutation in epithelioid glioblastoma and concomitant low-grade astrocytoma. *Neuropathology* **37**:58–63.

23. Mistry M, Zhukova N, Merico D, Rakopoulos P, Krishnatry R, Shago M *et al* (2015) BRAF mutation and CDKN2A deletion define a clinically distinct subgroup of childhood secondary high-grade glioma. *J Clin Oncol* **33**:1015–1022.

24. Miyahara M, Nobusawa S, Inoue M, Okamoto K, Mochizuki M, Hara T (2016) Glioblastoma with rhabdoid features: report of two young adult cases and review of the literature. *World Neurosurg* **86**: 515.e1–515.e9.

25. Nagai S, Kurimoto M, Ishizawa S, Hayashi N, Hamada H, Kamiyama H, Endo S (2009) A rare astrocytic tumor with rhabdoid features. *Brain Tumor Pathol* **26**:19–24.

26. Nagaishi M, Nobusawa S, Yokoo H, Sugiura Y, Tsuda K, Tanaka Y *et al* (2016) Genetic mutations in high grade gliomas of the adult spinal cord. *Brain Tumor Pathol* **33**:267–269.

27. Nakazato Y, Ishizeki J, Takahashi K, Yamaguchi H, Kamei T, Mori T (1982) Localization of S-100 protein and glial fibrillary acidic protein-related antigen in pleomorphic adenoma of the salivary glands. *Lab Invest* **46**:621–626.

28. Nobusawa S, Hirato J, Kurihara H, Ogawa A, Okura N, Nagaishi M *et al* (2014) Intratumoral heterogeneity of genomic imbalance in a case of epithelioid glioblastoma with BRAF V600E mutation. *Brain Pathol* **24**:239–246.

29. Nobusawa S, Lachuer J, Wierinckx A, Kim YH, Huang J, Legras C *et al* (2010) Intratumoral patterns of genomic imbalance in glioblastomas. *Brain Pathol* **20**:936–944.

30. Schiffman JD, Hodgson JG, VandenBerg SR, Flaherty P, Polley MY, Yu M *et al* (2010) Oncogenic BRAF mutation with CDKN2A inactivation is characteristic of a subset of pediatric astrocytomas. *Cancer Res* **70**:512–519.

31. Schindler G, Capper D, Meyer J, Janzarik W, Omran H, Herold-Mende C *et al* (2011) Analysis of BRAF V600E mutation in 1,320 nervous system tumors reveals high mutation frequencies in pleomorphic xanthoastrocytoma, ganglioglioma and extra-cerebellar pilocytic astrocytoma. *Acta Neuropathol* **121**:397–405.

32. Schwab CJ, Jones LR, Morrison H, Ryan SL, Yigittop H, Schouten JP, Harrison CJ (2010) Evaluation of multiplex ligation-dependent probe amplification as a method for the detection of copy number abnormalities in B-cell precursor acute lymphoblastic leukemia. *Genes Chromosomes Cancer* **49**:1104–1113.

33. Tagawa H, Karnan S, Suzuki R, Matsuo K, Zhang X, Ota A *et al* (2005) Genome-wide array-based CGH for mantle cell lymphoma: identification of homozygous deletions of the proapoptotic gene BIM. *Oncogene* **24**:1348–1358.

34. Tanaka S, Nakada M, Nobusawa S, Suzuki SO, Sabit H, Miyashita K, Hayashi Y (2014) Epithelioid glioblastoma arising from pleomorphic xanthoastrocytoma with the BRAF V600E mutation. *Brain Tumor Pathol* **31**:172–176.

35. Vaubel RA, Caron AA, Yamada S, Decker PA, Eckel Passow JE, Rodriguez FJ *et al* (2017) Recurrent copy number alterations in low-grade and anaplastic pleomorphic xanthoastrocytoma with and without BRAF V600E mutation. *Brain Pathol* [Epub ahead of print; doi: 10.1111/bpa.12495].

36. Watanabe K, Tachibana O, Sato K, Yonekawa Y, Kleihues P, Ohgaki H (1996) Overexpression of the EGF receptor and p53 mutations are mutually exclusive in the evolution of primary and secondary glioblastomas. *Brain Pathol* **6**:217–224.

37. Watanabe T, Nobusawa S, Kleihues P, Ohgaki H (2009) IDH1 mutations are early events in the development of astrocytomas and oligodendrogliomas. *Am J Pathol* **174**:1149–1153.

38. Weber RG, Hoischen A, Ehrler M, Zipper P, Kaulich K, Blaschke B *et al* (2007) Frequent loss of chromosome 9, homozygous CDKN2A/p14(ARF)/CDKN2B deletion and low TSC1 mRNA expression in pleomorphic xanthoastrocytomas. *Oncogene* **26**: 1088–1097.

39. Yokoo H, Kinjo S, Hirato J, Nakazato Y (2006) Fluorescence in situ hybridization targeted for chromosome 1p of oligodendrogliomas (in Japanese). *Rinsho Kensa* **50**:761–766.

40. Yokoo H, Nobusawa S, Takebayashi H, Ikenaka K, Isoda K, Kamiya M *et al* (2004) Anti-human Olig2 antibody as a useful immunohistochemical marker of normal oligodendrocytes and gliomas. *Am J Pathol* **164**:1717–1725.

41. Zacher A, Kaulich K, Stepanow S, Wolter M, Köhrer K, Felsberg J *et al* (2017) Molecular diagnostics of gliomas using next generation sequencing of a glioma-tailored gene panel. *Brain Pathol* **27**:146–159.

## SUPPORTING INFORMATION

Additional Supporting Information may be found in the online version of this article at the publisher's web-site:

**Table S1**. Copy number abberations (CNA) detected by array comparative genomic hybridization.

**Figure S1.** MLPA and FISH analysis. **A**. MLPA analysis shows *CDKN2A/B* homozygous deletion (dosage quotient < 0.4) both in oligoastrocytoma-like and E-GBM components of case 8. *IDH1/2* mutation or 1p/19q loss is not detected in either component. **B**. LOH of *ODZ3* is detected in recurrent E-GBM but not in primary PXA of case 2, using a red probe targeting *ODZ3* and a reference probe labeled in green. E-GBM; epithelioid glioblastoma, PXA; pleomorphic xanthoastrocytoma, MLPA; multiplex ligation-dependent probe amplification, FISH; fluorescence in situ hybridization, LOH; loss of heterozygosity.